OsteoArthritis and Cartilage (2007) **15**, 1093–1096
© 2007 Osteoarthritis Research Society International. Published by Elsevier Ltd. All rights reserved.
doi:10.1016/j.joca.2007.03.011

Osteoarthritis and Cartilage

International Cartilage Repair Society

OA OSTEOARTHRITIS

Brief report
Extracorporeal shock wave therapy improves motor dysfunction and pain originating from knee osteoarthritis in rats

N. Ochiai M.D., Ph.D.†*, S. Ohtori M.D., Ph.D.†, T. Sasho M.D., Ph.D.†, K. Nakagawa M.D., Ph.D.†, K. Takahashi M.D., Ph.D.†, N. Takahashi M.D., Ph.D.†, R. Murata M.D., Ph.D.†, K. Takahashi M.D., Ph.D.†, H. Moriya M.D., Ph.D.†, Y. Wada M.D., Ph.D.‡ and T. Saisu M.D., Ph.D.§

† *Department of Orthopedic Surgery, Graduate School of Medicine, Chiba University, Japan*

‡ *Department of Orthopaedic Surgery, Teikyo University Ichihara Hospital, Japan*

§ *Division of Orthopedic Surgery, Chiba Children's Hospital, Japan*

Summary

Objective: Although there have been several reports on the use of extracorporeal shock wave therapy (ESWT), the efficacy of ESWT for knee osteoarthritis (OA) has not been clarified. The aim of this study is to investigate the effect of ESWT on OA in a rat knee model.

Methods: The rats were divided into three groups: (1) control, (2) OA, and (3) ESWT (knee OA + shock wave therapy). Behavioral analysis consisted of measuring the duration of walking on a treadmill. The expression of calcitonin gene-related peptide (CGRP) in dorsal root ganglion (DRG) neurons innervating the knee using immunohistochemistry was examined in the three groups at their peak time point on the treadmill.

Results: Walking duration was significantly extended 4, 7 and 14 days after ESWT in rats with knee OA (peak time point: 4 days), again decreasing by days 21 and 28. Immunohistochemical studies revealed that the OA group had significantly higher percentages of CGRP positive neurons in the DRG than were found in the control group. In addition, ESWT reduced the ratio of CGRP positive DRG neurons in the OA model.

Conclusion: The improvement in walking ability and the reduction of CGRP positive neurons in DRG indicates that ESWT is a useful treatment for knee OA.
© 2007 Osteoarthritis Research Society International. Published by Elsevier Ltd. All rights reserved.

Key words: Extracorporeal shock wave therapy, Dorsal root ganglion, Calcitonin gene-related peptide, Knee osteoarthritis.

Introduction

Chronic pain while walking and functional limitation are some of the clinical manifestations of the osteoarthritis (OA) knee in many of the elderly. The goal of management of the patient with OA is control of pain and improvement in function and quality of life.

The neuropeptide calcitonin gene-related peptide (CGRP) is expressed by nociceptors and is thought to play a role in the sensation of joint pain[1]. CGRP has been shown by immunohistochemistry to be expressed in nerve fibers supplying the rat knee at both the level of the dorsal root ganglion (DRG)[2] and locally in the knee[3]. Increased synthesis of CGRP peptides in DRG may play a role in the pathogenesis of chronic arthritis[4]. A significant decrease in the number of CGRP-immunoreactive (ir) DRG neurons was found after rofecoxib treatment that was also correlated with behavioral improvement[4].

Recently, extracorporeal shock wave therapy (ESWT) has been proven effective for pain relief and for stimulating healing of chronic tendinoses[5]. Although it has been reported that ESWT is effective therapy for patients suffering from several kinds of orthopedic disorders[5,6], there have been no studies to reveal its effectiveness for the treatment of knee OA. The aim of this study is to identify the effectiveness of ESWT for an animal model of knee OA. Walking duration on a treadmill was analyzed before and after treatment. In addition, immunohistochemistry was used to observe changes in CGRP expression in the DRG neurons innervating the knee joints in rat OA model.

Methods

ANIMALS

The experimental protocol was conducted in accordance with the guidelines of the Ethics Review Committee of Chiba University for Animal Experimentation. Thirty-three male Sprague Dawley rats (Japan SLC, Japan) weighing approximately 250 g were used for these studies. Surgery, application of ESWT, and control study were carried out under general anesthesia with 40 mg/kg sodium pentobarbital. Fifteen rats were used for behavioral studies and 18 were used for immunohistochemistry studies.

The OA model was induced by transection of both the anterior cruciate ligament and medial collateral ligament with microscissors and resection of the medial meniscus as previously described[7]. In control-operated animals, wounds were closed after subluxation of the patella. All the rats were allowed to move freely in plastic cages until 10 weeks post-surgery.

*Address correspondence and reprint requests to: Nobuyasu Ochiai, Department of Orthopedic Surgery, Graduate School of Medicine, Chiba University, 1-8-1 Inohana, Chuo-ku, Chiba 260-8670, Japan. Tel: 81-43-226-2117; Fax: 81-43-226-2116; E-mail: nobunobu1215@yahoo.co.jp

Received 23 August 2006; revision accepted 12 March 2007.

BEHAVIORAL TEST

Three control rats and 12 knee OA rats that were divided into two groups were used for behavioral analysis: (1) control (three rats); (2) OA (six rats); and (3) ESWT (knee OA and ESWT) (six rats) groups. An accelerating Rota-Rod Treadmill (Ugo Basile, Italy) was used for behavioral tests as previously described[8]. Walking duration was measured before treatment and 4, 7, 14, 21, and 28 days after treatment in the ESWT group. One thousand shock wave impulses with an energy flux density of 0.08 mJ/mm^2 were applied at a frequency of 4 Hz (Dornir MedTech.; Epos, Germany) to the left medial side of the knees of six OA model rats in the ESWT group. Only control and OA groups were anesthetized without application of shock waves. Walking time duration measurements were taken three times at 5-min intervals each day. The average was calculated and used as the duration time. These times were analyzed with a two-way analysis of variance (ANOVA) followed by a Bonferroni *post hoc* test. A P value less than 0.05 was considered statistically significant.

IMMUNOHISTOCHEMISTRY FOR CGRP IN DRG NEURONS

Eighteen animals were divided into three groups: (1) control (six knees); (2) OA (six knees); and (3) ESWT (six knees). A medial para-patellar incision (approximately 5 mm) was made with the leg held in an extended position. A perforation of approximately 0.5 mm in depth was made on the medial side of the knee using a 27-gauge needle and 50 μl of 10% w/v Fluoro-Gold crystals (FG; Fluorochrome, Denver, CO) were inserted. Ten days after the application of FG, ESWT was applied to six OA rats (ESWT group) in the same manner as described above. Only the control and OA groups were anesthetized without application of shock waves. All rats were perfused 14 days after application of FG as previously described[9]. The left DRGs from L2 to L6 were harvested. The DRGs were immersed in fixative overnight at 4°C, after which they were transferred to 20% sucrose overnight[9]. Serial sections (40 μm thick) were prepared from the DRGs using a cryostat and mounted on poly-L-lysine-coated slides.

The sections were treated for 90 min at room temperature in blocking solution (0.01 M phosphate buffered saline (PBS) containing 0.3% Triton X-100 and 1% normal goat serum). The DRGs were then incubated overnight at room temperature with rabbit anti-CGRP (1:800; ImmunoStar, Hudson, WI) diluted with blocking solution for 20 h at 4°C. After washing three times with PBS, sections were incubated for 2 h in an Alexa Fluoro 488 with conjugated anti-rabbit IgG (1:250; Molecular Probes, Eugene, OR). The number of FG-labeled, and FG-labeled CGRP-ir DRG neurons were counted using a fluorescence microscope.

The major categories subjected to analysis were: (1) the average number of FG-labeled neurons; and (2) the percentage of FG-labeled neurons that expressed CGRP (CGRP-ir neurons), at three random sections for each harvested DRG. Statistical analyses of these values were carried out using a Mann–Whitney Rank sum test. A P value less than 0.05 was considered statistically significant.

Results

BEHAVIORAL TEST

The average walking duration times for control, ESWT and OA groups are shown in Fig. 1. Walking duration time of the ESWT and OA groups at time 0 was significantly shorter compared to the control group ($P < 0.05$). Walking duration was significantly increased by 4, 7, and 14 days after ESWT ($P < 0.05$). However, there was no significant difference on the twenty-first and twenty-eighth days compared to the duration of walking before ESWT. Furthermore, walking duration of the ESWT group was significantly extended 4, 7, and 14 days after ESWT ($P < 0.05$) compared to the OA group at each time point. However, there was no significant difference on the twenty-first and twenty-eighth days. Therefore, ESWT was effective for 14 days post-treatment. Fig. 1 shows that peak walking duration time was 4 days post-treatment. Therefore DRGs were harvested on 4 days after ESWT for immunohistochemistry.

IMMUNOHISTOCHEMISTRY FOR CGRP

FG was retrogradely transported to the DRG neurons innervating the knee joint [Fig. 2(A, C, E)]. The FG-labeled neurons were distributed in the L2–L6 DRGs in all three groups. There was no significant difference in the average numbers of FG-labeled neurons among the three groups ($P > 0.05$). The average numbers of FG-labeled neurons were shown (control group 8.2 ± 3.8; OA group 8.2 ± 3.7; ESWT group 9.8 ± 4.7). Of the FG-labeled neurons innervating the knee joints, the ratios of CGRP-ir neurons in control (44.9 ± 17.6%) and ESWT groups (43.8 ± 12.7%) were significantly less than the ratio in the OA group (65.7 ± 16.3%) ($P < 0.0001$) [Fig. 2(B, D, F)]. ESWT reduced this ratio in those neurons in the DRGs of the OA model. The numbers and ratio for each group are shown as average ± SD.

Discussion

This study showed depression of CGRP in the DRG neurons after the treatment by ESWT. The abundance of CGRP-ir free nerve endings in the synovium corresponds to the location of pain in knee OA[10]. Increasing the CGRP

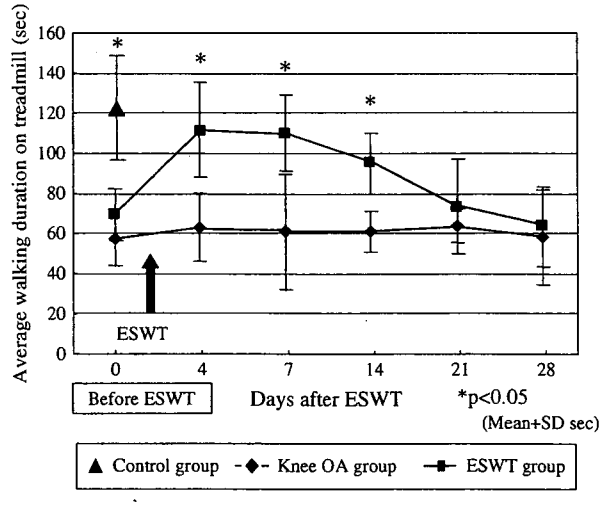

Fig. 1. Average walking duration on treadmill. The increase in walking duration was statistically significant on days 4, 7, and 14 after the application of shock waves. But there was no significant difference on day 21 or day 28. Asterisks indicate statistical significance (*$P < 0.05$) compared to before ESWT and to the knee OA group. Each point represents the mean value ± SD for the control, knee OA, and ESWT groups.

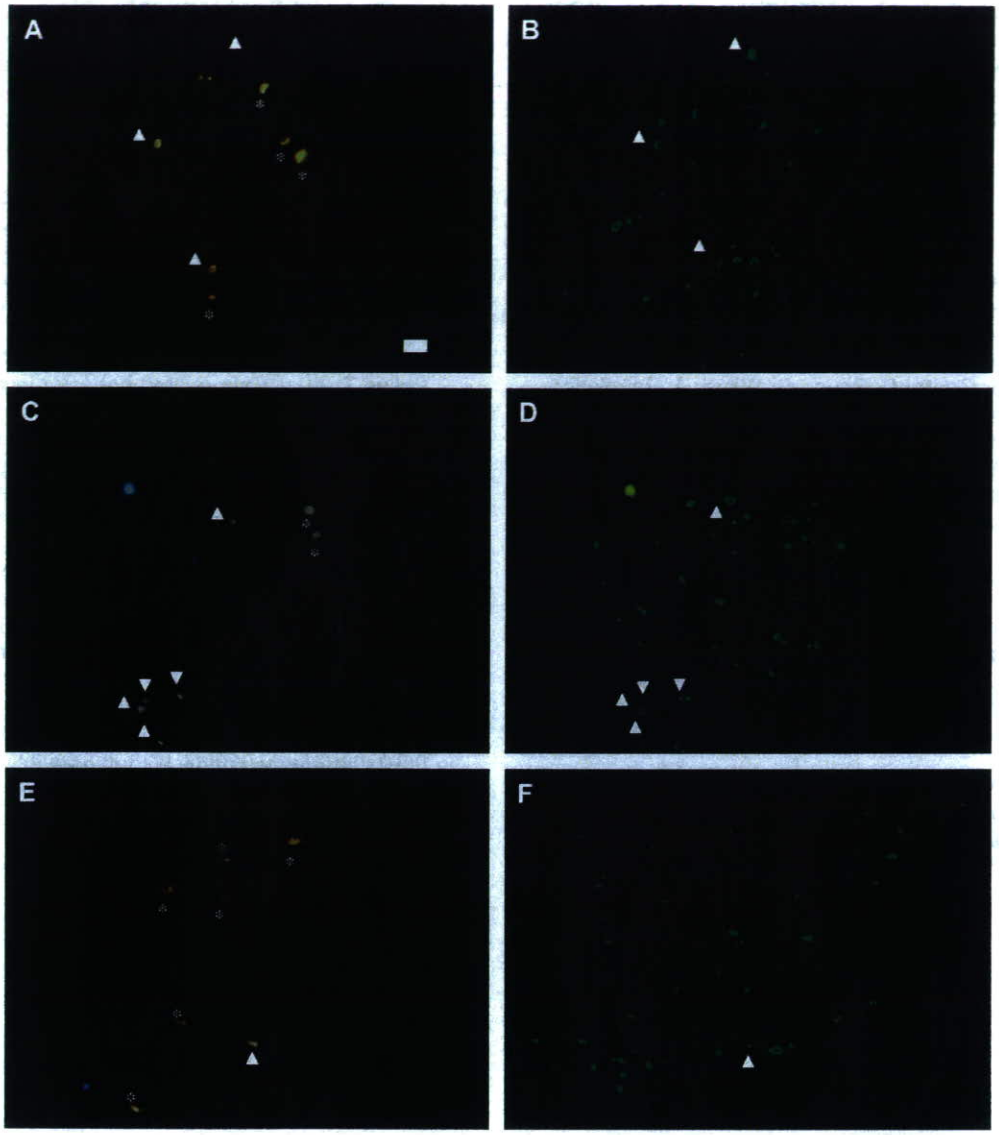

Fig. 2. Fluorescence photomicrographs of DRG neurons. Fluorescence photomicrographs showing DRG neurons labeled following FG application to the knee (A, C, E). B, D and F show CGRP-ir DRG neurons. A and B are from the same section of L4 DRG in the control group, C and D are from the same section of L4 DRG in the OA group, and E and F are from the same section of L4 DRG in the ESWT group. Arrowheads indicate FG-labeled neurons that are CGRP-ir and asterisks indicate FG-labeled neurons that are CGRP-negative. Numbers of FG-labeled, CGRP-ir neurons decrease in control and ESWT groups. The scale bar is 100 μm.

expression in the DRG[2] corresponds to robust hyperalgesia in the OA knee model[11]. A CGRP antagonist reduces the response of hyperexcitable spinal neurons to both innocuous and noxious pressure applied to the inflamed joint[12]. After sciatic nerve sectioning in the rat, CGRP-ir in DRG neurons was decreased[13], and the rats demonstrated analgesia to heat stimuli. Furthermore, there was a significant decrease in the number of CGRP-ir DRG neurons in rofecoxib-treated rats, which was also correlated with behavioral data where hypersensitivity was significantly reduced[4]. We previously reported that application of shock waves to normal rat skin reduced the number of CGRP-ir sensory nerve fibers[9] in the foot pad with the reduction of CGRP expression in DRG neurons[14]. However, one of the limitations of those studies was that the shock waves were applied under normal conditions. Whether the same mechanism would operate under pathological conditions is unknown.

Behavioral examination also revealed the effectiveness of ESWT. Walking duration was extended during a 14-day period after ESWT. This result is consistent with reinnervation of free nerve endings 2 weeks after ESWT[9]. A limitation of this study is that changes in the number of CGRP-ir DRG neurons were not examined over time. The number of CGRP-ir DRG neurons may increase again by day 21, as found for nerve fibers in rat skin[9]. Another limitation of this study is that we did not examine the anatomical joint outcome after ESWT. Further study is necessary to clarify the long-term anatomical outcome.

Although there are many reports regarding the use of ESWT to treat orthopedic disorders[5,6], there were none specifically for knee OA. Since ESWT does not cause damage to the joint cartilage of growing rabbits[15], side effects are anticipated to be rare. Therefore, the use of ESWT is recommended for knee OA prior to surgical treatment.

The current finding of reduced CGRP expression in DRG neurons provides, at least in part, possible explanation for pain relief following ESWT in knee OA, with a concomitant improvement in walking ability lasting for 2 weeks. Therefore, these data show that ESWT may be a useful treatment for knee OA.

References

1. He X, Schepelmann K, Schaible HG, Schmidt RF. Capsaicin inhibits responses of fine afferents from the knee joint of the cat to mechanical and chemical stimuli. Brain Res 1990;530:147–50.
2. Fernihough J, Gentry C, Bevan S, Winter J. Regulation of calcitonin gene-related peptide and TRPV1 in a rat model of osteoarthritis. Neurosci Lett 2005;388:75–80.
3. Schwab W, Bilgicyildirim A, Funk RHW. Microtopography of the autonomic nerves in the rat knee: a fluorescence microscopic study. Anat Rec 1997;247:109–81.
4. Staton PC, Wilson AW, Bountra C, Chessell IP, Day NC. Changes in dorsal root ganglion CGRP expression in a chronic inflammatory model of the rat knee joint: differential modulation by rofecoxib and paracetamol. Eur J Pain 2007;11:283–9.
5. Rompe JD, Hope C, Kullmer K, Heine J, Burger R. Analgesic effect of extracorporeal shock-wave therapy on chronic tennis elbow. J Bone Joint Surg Br 1996; 78:233–7.
6. Rompe JD, Rumler F, Hopf C, Nafe B, Heine J. Extracorporeal shock wave therapy for calcifying tendinitis of the shoulder. Clin Orthop 1995;321:196–201.
7. Hayami T, Pickarski M, Zhuo Y, Wesolowski GA, Rodan GA, Duong LT. Characterization of articular cartilage and subchondral bone changes in the rat anterior cruciate ligament transection and meniscectomized models of osteoarthritis. Bone 2006;38:234–43.
8. Linda SF, Christine M, Jane P, Jon DL. Dissociation of antinociceptive and motor effects of supraspinal opioid agonists in the rat. Brain Res 1991;563:123–6.
9. Ohtori S, Inoue G, Mannoji C, Saisu T, Takahashi K, Mitsuhashi S, *et al.* Shock wave application to rat skin induces degeneration and reinnervation of sensory nerve fibres. Neurosci Lett 2001;315:57–60.
10. Saito T, Koshino T. Distribution of neuropeptides in synovium of the knee with osteoarthritis. Clin Orthop 2000;376:172–82.
11. Fernihough J, Gentry C, Malcangio M, Fox A, Rediske J, Pellas T, *et al.* Pain related behavior in two models of osteoarthritis in the rat knee. Pain 2004;112:83–93.
12. Neugebauer V, Rumenapp P, Schaible HG. Calcitonin gene-related peptide is involved in the spinal processing of mechanosensory input from the rat's knee joint and in the generation and maintenance of hyperexcitability of dorsal horn-neurons during development of acute inflammation. Neuroscience 1996;71:1095–109.
13. Doughty SE, Atkinson ME, Shehab SA. A quantitative study of neuropeptide immunoreactive cell bodies of primary afferent sensory neurons following rat sciatic nerve peripheral axotomy. Regul Pept 1991;35:59–72.
14. Takahashi N, Wada Y, Ohtori S, Saisu T, Moriya H. Application of shock wave to rat skin decreases calcitonin gene-related peptide immunoreactivity in dorsal root ganglion neurons. Auton Neurosci 2003;107:81–94.
15. Vaterlein N, Lussenhop S, Hahn M, Delling G, Meiss AL. The effect of extracorporeal shock waves on joint cartilage – an *in vivo* study in rabbits. Arch Orthop Trauma Surg 2000;120:403–6.

J Orthop Sci (2007) 12:265–273
DOI 10.1007/s00776-007-1111-8

JOURNAL OF
ORTHOPAEDIC SCIENCE
©The Japanese Orthopaedic Association

Original article

Evaluation of reparative cartilage after autologous chondrocyte implantation for osteochondritis dissecans: histology, biochemistry, and MR imaging

TAKURO MORIYA[1,3], YUICHI WADA[2], ATSUYA WATANABE[1,3], TAKAHISA SASHO[1], KOICHI NAKAGAWA[1], PIERRE MAINIL-VARLET[3], and HIDESHIGE MORIYA[1]

[1]Department of Orthopaedic Surgery, Graduate School of Medicine, Chiba University, 1-8-1 Inohana, Chuo-ku, Chiba 260-8677, Japan
[2]Department of Orthopaedic Surgery, Teikyo University Chiba Medical Center, Ichihara, Japan
[3]Institute of Pathology, University of Bern, Bern, Switzerland

Abstract

Background. The aim of this study was to investigate the biochemical properties, histological and immunohistochemical appearance, and magnetic resonance (MR) imaging findings of reparative cartilage after autologous chondrocyte implantation (ACI) for osteochondritis dissecans (OCD).

Methods. Six patients (mean age 20.2 ± 8.8 years; 13–35 years) who underwent ACI for full-thickness cartilage defects of the femoral condyle were studied. One year after the procedure, a second-look arthroscopic operation was performed with biopsy of reparative tissue. The International Cartilage Repair Society (ICRS) visual histological assessment scale was used for histological assessment. Biopsied tissue was immunohistochemically analyzed with the use of monoclonal antihuman collagen type I and monoclonal antihuman collagen type II primary antibodies. Glycosaminoglycan (GAG) concentrations in biopsied reparative cartilage samples were measured by high performance liquid chromatography (HPLC). MR imaging was performed with T_1- and T_2-weighted imaging and three-dimensional spoiled gradient-recalled (3D-SPGR) MR imaging.

Results. Four tissue samples were graded as having a mixed morphology of hyaline and fibrocartilage while the other two were graded as fibrocartilage. Average ICRS scores for each criterion were (I) 1.0 ± 1.5; (II) 1.7 ± 0.5; (III) 0.6 ± 1.0; (IV) 3.0 ± 0.0; (V) 1.8 ± 1.5; and (VI) 2.5 ± 1.2. Average total score was 10.7 ± 2.8. On immunohistochemical analysis, the matrix from deep and middle layers of reparative cartilage stained positive for type II collagen; however, the surface layer did not stain well. The average GAG concentration in reparative cartilage was 76.6 ± 4.2 μg/mg whereas that in normal cartilage was 108 ± 11.2 μg/mg. Common complications observed on 3D-SPGR MR imaging were hypertrophy of grafted periosteum, edema-like signal in bone marrow, and incomplete repair of subchondral bone at the surgical site. Clinically, patients had significant improvements in Lysholm scores.

Conclusions. In spite of a good clinical course, reparative cartilage after ACI had less GAG concentration and was inferior to healthy hyaline cartilage in histological and immunohistochemical appearance and on MRI findings.

Offprint requests to: T. Moriya
Received: August 14, 2006 / Accepted: January 16, 2007

Introduction

Articular cartilage is composed of hyaline cartilage containing a relatively small number of chondrocytes embedded in abundant extracellular matrix materials such as type II collagen and proteoglycan.[1] Articular cartilage has limited intrinsic repair capacity, and damage to cartilage or mechanical damage to the joint surface can be a risk factor for more extensive joint damage.[2] Over the past 10 years, autologous chondrocyte implantation (ACI) has been a widely used technique for treatment of articular cartilage lesions, and good to excellent clinical results have been reported.[3,4] However, several investigators have conducted histological and/or biochemical analyses of ACI repair sites and reported that the reparative cartilage was not always identical to native hyaline cartilage found in normal articular cartilage.[5] In previous reports, reparative cartilage was assessed with qualitative methods: the presence of key components such as proteoglycan and type II collagen was observed in reparative tissues.[6,7] However, only a few reports have included quantitative biochemical analysis of such matrix components. Biochemical analysis of extracellular matrix that can characterize the nature of reparative and native articular cartilage is considered to be essential to assess reparative tissue and predict prognosis after ACI. We hypothesized that reparative tissue after ACI would contain abundant proteoglycan but might have less than native cartilage. In addition, we were interested in exploring some adverse effects of ACI that have been reported, e.g., graft failure, delamination, and tissue hypertrophy.[8]

The aim of this study was to assess the efficacy of ACI as a cartilage repair method by use of histological as-

sessment such as general histology and immunohistochemistry, biochemical quantitative analysis, magnetic resonance (MR) imaging, clinical evaluation, and macroscopic assessment on follow-up arthroscopy.

Materials and methods

This study was approved by the Ethics Review Committee of Chiba University Hospital. The patients gave consent for ACI as a two-stage process, with a follow-up arthroscopy procedure including biopsy approximately 1 year after the second stage of the procedure. Additionally, patients were informed that data derived from their procedures would be submitted for publication, and they gave their consent.

Patients

ACI was performed in six male patients (mean age, 20.2 ± 8.8 years; age range, 13–35 years) for osteochondritis dissecans (OCD) at a femoral condyle (five medial, one lateral). All were full-thickness cartilage defects graded as ICRS (International Cartilage Repair Society) OCD: IV and ICRS Grade 4: severely abnormal.[9] The size of the lesions ranged from 400 to 1280 mm^2 (mean, 596 ± 345 mm^2).

ACI procedure

A small biopsy of articular cartilage was collected from a non-weight-bearing area (e.g., trochlear cartilage). Biopsy specimens were sent to Genzyme (Carticel Service, Genzyme, Cambridge, MA, USA) for processing and culturing. After enzymatic digestion of the tissue and 3-week cultivation of the chondrocytes in culture medium including fetal bovine serum and gentamicin, patients were readmitted to our hospital for the second stage of the procedure. To prepare for chondrocyte implantation, a medial parapatellar arthrotomy was performed. The osteochondral lesion was debrided with minimum bleeding, and thrombin was given to stop bleeding from subchondral bone tissue. A periosteal flap was harvested from the proximal medial tibia and was fitted and sutured to the surrounding rim of cartilage with 5-0 Vicryl. The periosteal flap was sealed to the rim with fibrin glue except for one upper corner, within which the cultured chondrocytes were injected into the defect. After chondrocyte injection beneath the periosteal flap, the remaining defect between the periosteal flap and rim was sutured with 5-0 Vicryl and sealed with fibrin glue. Each defect received approximately 1.6 million cells/cm^2 of cultured chondrocytes.

Rehabilitation

The rehabilitation schedule for each patient included active and passive movement, muscle training, and weight-bearing exercise. Patients began physiotherapy with 0°–30° angle of continuous passive motion beginning 6 h after surgery. The range of motion was gradually increased until 12 weeks, culminating in full flexion. Each patient remained non-weight-bearing for the 1st to 4th postoperative week, with partial weight-bearing exercise beginning after the 4th week. By the 12th postoperative week, patients had progressed to walking with full weight-bearing. Sports activity was gradually increased after 6 months; however, hard sporting activity was allowed only after 12 months.

Tissue biopsies

At the 1-year (12.4 ± 0.7 months) follow-up, arthroscopic assessments were performed for all patients, and tissue biopsies were taken from the center of the ACI repair site and also from a normal area at the lateral side of the femoral condyle (the latter as controls). Full-depth cores of cartilage and subchondral bone were obtained from all six patients. Biopsies were taken from the center of the graft region using an 11-gauge biopsy needle (Trapsystem MDTECH, Gainesville, FL, USA). The cores were taken as closely as possible to a 90° angle to the articular surface. Biopsy samples were used for histological, immunohistochemical, and biochemical analyses.

Histological assessment

For general histology, 7-μm-thick frozen sections were stained with hematoxylin and eosin (H&E), safranin-O (0.5% in 0.1 M sodium acetate, pH 4.6, for 30 s), and Masson-trichrome stain.

The ICRS Visual Histological Assessment Scale[10] (Table 1) was used to grade the reparative tissue samples. The biopsy specimens were evaluated by a skilled cartilage research pathologist, who used both polarized and plain light microscopy to assess collagen organization and morphology of each sample.

For immunohistochemical analysis, the following primary antibodies were used: mouse monoclonal antihuman collagen type I antibody and mouse monoclonal antibody to collagen type II (Immunodiagnostika und Biotechnologie, Berlin, Germany).

Biochemical assessment

Concentrations of GAG in reparative and native cartilage samples from four patients were measured with high performance liquid chromatography (HPLC). The

Table 1. International Cartilage Repair Society (ICRS) Visual Histological Assessment scale

Feature	Score
I. Surface	
Smooth/continuous	3
Discontinuities/irregularities	0
II. Matrix	
Hyaline	3
Mixture: hyaline/fibrocartilage	2
Fibrocartilage	1
Fibrous tissue	0
III. Cell distribution	
Columnar	3
Mixed/columnar clusters	2
Clusters	1
Individual cells/disorganized	0
IV. Cell population viability	
Predominantly viable	3
Partially viable	1
<10% viable	0
V. Subchondral bone	
Normal	3
Increased remodeling	2
Bone necrosis/granulation tissue	1
Detached/fracture/callus at base	0
VI. Cartilage mineralization (calcified cartilage)	
Normal	3
Abnormal/inappropriate location	0

HPLC procedures were performed in accordance with the method described by Shinmei et al.[11]

MR imaging and assessment

MR imaging was performed with a 1.5-Tesla magnet (Signa Horizon General Electronic, Milwaukee, WI, USA) using a knee coil preoperatively and at 1 year postoperatively. Imaging was performed in the sagittal plane, and a series of T_1-weighted and T_2-weighted images were obtained as routine sequences. In addition, fat-suppressed three-dimensional spoiled gradient-recalled (3D-SPGR) sequences[12] were performed to obtain more morphological details, with 1.5-mm slice thickness, repetition time of 52 ms, echo time of 10 ms, flip angle of 60°, field of view 130 × 130 mm, and matrix of 512 × 512 pixels. Imaging was performed using the same MR scanner, coil, and sequence each time.

Evaluation of MR images was performed based on the scoring systems used by Sally Roberts (Roberts et al.[5]) (Table 2) and by Henderson et al.[13] (Table 3), by a skilled musculoskeletal radiologist who was unaware of the histological evaluation.

Clinical evaluation

The clinical status of patients was evaluated before ACI and 1 year after the operation using the Lysholm score[14] and the overall Brittberg clinical grading score.[1]

Table 2. Magnetic resonance (MR) imaging score applied by Roberts et al.[5]

Feature	Score
I. Surface integrity and contour	1 = normal or near normal, 0 = abnormal
II. Cartilage signal in graft region	1 = normal or near normal, 0 = abnormal
III. Cartilage thickness	1 = normal or near normal, 0 = abnormal
IV. Changes in underlying bone	1 = normal or near normal, 0 = abnormal
Maximum total possible	4 (minimum: 0 is the worst)

Table 3. MR imaging score applied by Henderson et al.[13]

Feature	Score
I. Fill of the repair site	Complete = 1, >50% of the defect = 2 <50% of the defect = 3 Full-thickness defect = 4
II. Signal at the repair site	Normal = 1, Nearly normal = 2, Abnormal = 3, Absent = 4
III. Bone marrow edema	Absent = 1, Mild = 2. Moderate = 3, Severe = 4
IV. Joint effusion	Absent = 1, Mild = 2. Moderate = 3, Severe = 4
Minimum total possible	4 (maximum: 16 is the worst)

Macroscopic assessment

Arthroscopic assessment of reparative tissue was performed based on the ICRS cartilage repair assessment (Protocol A)[9] by a skilled orthopedic surgeon. The scoring system assigns a maximum of 12 points and is based on the degree of defect repair, integration into border zones, and macroscopic appearance.

Statistical analysis

A paired *t* test was used for statistical evaluation of both the GAG concentrations and the assessment of the Lysholm score. A significant difference was defined as $P < 0.05$.

Results

Histology

Four samples displayed mixed morphology of hyaline cartilage and fibrocartilage, in which several rounded chondrocytes were observed in typical lacunae. In contrast, the two remaining samples showed only fibrocartilage (Table 4). In the samples graded as fibrocartilage, however, there were several small islands that resembled hyaline-like cartilage. In the samples with mixed morphology (Fig. 1a,b), half or more of the matrix stained positive for proteoglycans with safranin-O (Fig. 1c). Positive safranin-O staining was observed throughout the matrix except for the fibrous tissue on the sur-

Table 4. Details of individuals, their histology scores, and GAG concentrations

Patient number	Age	Sex	Location of defect	Size of defect (mm^2)	ICRS Visual Histological Assessment Scale							GAG concentration	
					I	II	III	IV	V	VI	Total	ACI (μg/mg)	Control (μg/mg)
1	16	M	MFC	437	0	1	0	3	0	3	7	N/A	N/A
2	35	M	MFC	500	0	2	2	3	3	0	10	77	97
3	27	M	MFC	1280	0	2	0	3	0	3	8	N/A	N/A
4	15	M	MFC	400	3	1	0	3	2	3	12	81	115
5	15	M	LFC	361	3	2	0	3	3	3	14	78	120
6	15	M	MFC	600	0	2	2	3	3	3	13	71	100

ICRS, International Cartilage Repair Society; GAG, glycosaminoglycans; ACI, autologous chondrocyte implantation; MFC, medial femoral condyle; LFC, lateral femoral condyle; N/A. not available

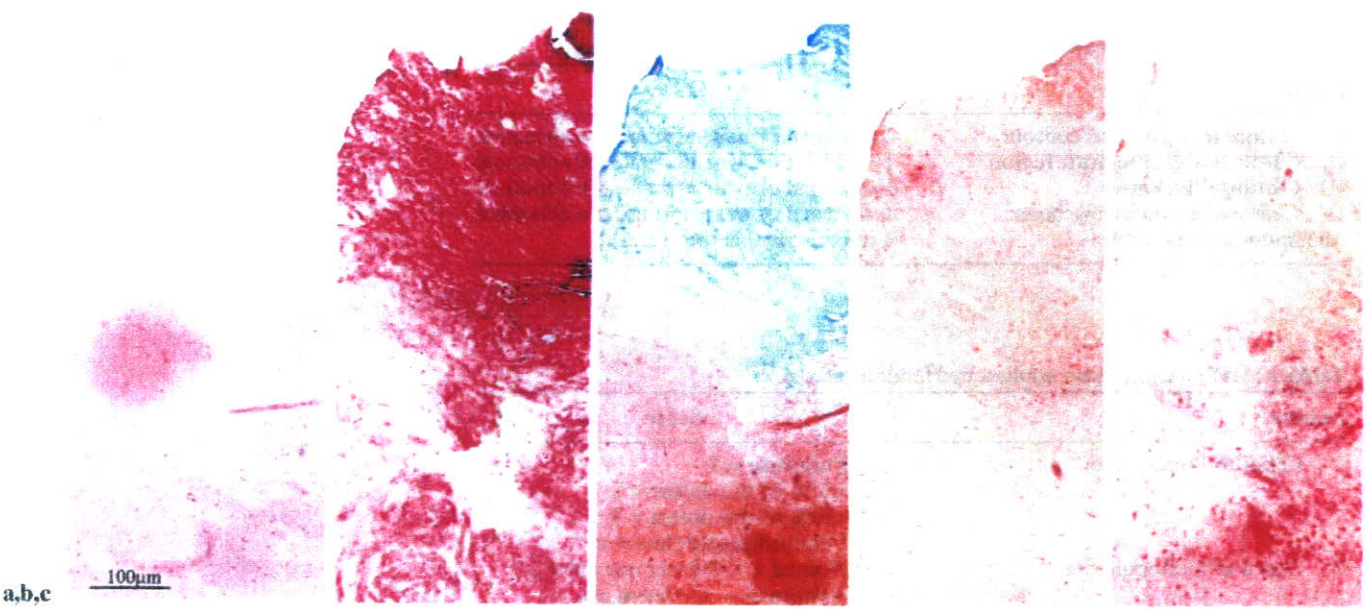

Fig. 1. Histology and immunohistochemistry of sample 5. **a** With hematoxylin and eosin staining, good cell viability was observed. **b** In the upper layer, roughly distributed collagen fibers were observed with Masson-trichrome staining. **c** With safranin-O staining (Saf-O), the deeper layer took up more stain because of the presence of proteoglycans. **d** The stain for type I collagen was observed in the upper part of the lesion; however, the stain for type II collagen was observed from the middle to deep layers (**e**)

face, and in three cases it was stronger in deeper zones than in superficial zones (Fig. 1c). Four samples showed surface irregularity, and in one of them the surface irregularity appeared to be caused by a remnant of periosteum, which was clearly demarcated from reparative cartilage originating from implanted chondrocytes. With respect to cell distribution, two samples showed a tendency to form columnar organization with some clusters of cells and were thus graded as mixed/columnar clusters. The other samples showed no organized distribution of cells. In contrast, all samples showed good viability of cell populations. Regarding the subchondral bone, one sample showed increased remodeling, two samples had a detached appearance, and three samples appeared normal. No sample showed a tidemark reorganization.

Immunohistochemistry

Type I collagen was slightly positive in all samples, but its distribution was more dispersed than that of type II collagen. In the samples graded as fibrocartilage, sparse immunoreactive type I collagen was observed throughout the matrix, whereas in samples with mixed morphology, the distribution of type I collagen was discrete and usually restricted to the uppermost regions (Fig. 1d). The tissue that appeared to be a periosteal remnant stained positive for type I collagen. All samples stained positive for type II collagen, which appeared throughout the reparative cartilage matrix, except in fibrous tissue derived from periosteum. Deep zones stained more strongly positive for type II collagen than upper zones (Fig. 1e). Additionally, deeper zones were more positive for type II than for type I collagen.

GAG concentration

The average GAG concentration in reparative tissue was 76.6 ± 4.2 μg/mg (range, 71–81 μg/mg), 71.5% ± 5.9% of the GAG concentration present in native cartilage, for which the average GAG concentration was 108 ± 11.2 μg/mg (range, 97–120 μg/mg). This difference in concentration was statistically significant ($P < 0.05$).

MR imaging

In all cases, the defect was completely filled with reparative tissue, which was iso-intense with the surrounding cartilage in four patients and of lower intensity than the surrounding cartilage in the remaining two patients (Table 5). In the sample with a deep osteochondral defect, signal intensity of reparative tissue was also almost homogeneously higher than that of underlying bone (Fig. 2a) on 3D-SPGR MR imaging. Hence, the reparative sample was considered cartilage-like tissue, and there was no finding of reparative subchondral bone in reparative tissue.

The surface of the reparative tissue was level with surrounding tissue in four patients; the remaining two patients showed overgrowth at the surface on 3D-SPGR MR imaging (Fig. 2b). The surface of subchondral bone was smooth and regular in three patients, but irregular in the other three cases. Three samples displayed bone marrow edema in subchondral bone at the repair site on T_1- and T_2-weighted images.

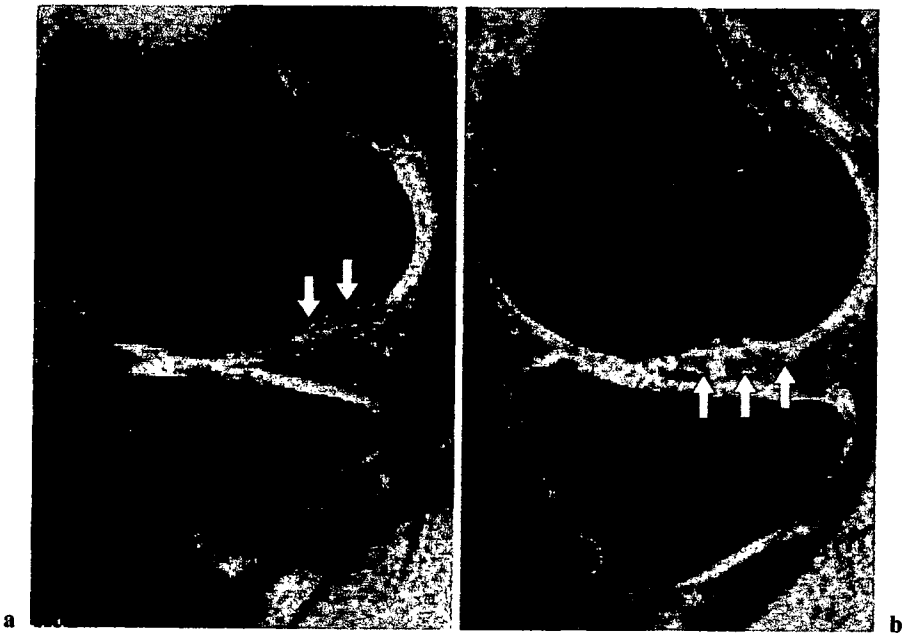

Fig. 2. Magnetic resonance (MR) images obtained 1 year after autologous chondrocyte implantation (ACI). **a** Cartilage filling in the original subchondral defect was identified on three-dimensional spoiled gradient-recalled (3D-SPGR) MR imaging (*arrows*). **b** The surface of the reparative cartilage showed some irregularity and overgrowth (*arrows*)

Table 5. Details of MRI score, Lysholm score, and arthroscopic assessment

Patient number	MRI score of Robert					MRI score of Henderson					Lysholm score		ICRS Cartilage Repair Assessment				
	I	II	III	IV	Total	I	II	III	IV	Total	Before ACI	1y after ACI	I	II	III	Total	Grade
1	0	0	0	1	1	1	2	1	1	5	74	95	4	4	2	10	II: Nearly Normal
2	0	1	0	0	1	1	1	2	1	5	64	96	4	4	3	11	II: Nearly Normal
3	0	1	0	1	2	1	1	1	1	4	66	99	4	4	3	11	II: Nearly Normal
4	1	1	0	0	2	1	1	2	1	5	56	91	4	4	4	12	I: Normal
5	1	1	0	1	3	1	1	1	1	4	76	100	4	4	3	11	II: Nearly Normal
6	0	0	1	0	1	1	2	2	1	6	71	100	4	4	3	11	II: Nearly Normal

ICRS cartilage repair assessment: (I) degree of defect repair, (II) integration to border zones, (III) macroscopic appearance. Grade: I, normal: 12P; II, nearly normal: 11-9P; III, abnormal: 7-4P; IV, severely abnormal: 3-1P

Clinical evaluation

One year after ACI, all patients had reduced knee pain and swelling, and locking sensation had disappeared. Before their operations, all patients had scored poorly on the overall Brittberg clinical grading score. One year after the operation, two patients scored as excellent and the other four scored as good. There was a significant improvement in the patients' Lysholm score, from a mean of 67.8 ± 7.4 points before surgery to a mean of 96.8 ± 3.5 points 1 year after ACI (see Table 5). Two patients showed full recovery of Lysholm scores. The other four patients complained of catching sensations and some difficulties with squatting or climbing stairs. However, after trimming of hypertrophied reparative tissue at the follow-up operation, catching sensations were diminished and the patients no longer complained of any pain or joint swelling. All patients returned to normal daily living and sports activities by 1 year after ACI.

Arthroscopy

One case was grade I on the ICRS cartilage repair assessment; the other five cases had grade II reparative cartilage with "a fibrillated surface" or "small, scattered fissures or cracks" (see Table 5). All patients had refilling of the defect; however, in three patients there was overgrowth of the graft. The patients who complained of an obvious catching sensation underwent trimming of the overgrown tissue. The tissue was similar in color and texture to the surrounding cartilage observed underneath the overgrown tissue.

Discussion

In many reports, ACI has been described as a safe and accepted technique for repair of articular cartilage lesions that can provide durable reparative tissue up to about 10 years after the procedure.[4] However, Roberts et al. reported that graft morphology of reparative cartilage after ACI varied from predominantly hyaline, through mixed, to predominantly fibrocartilage[5]; implantation effectiveness might be considered controversial. In addition, the adverse effects of graft failure, delamination, and hypertrophic tissue have been reported.[8] On the other hand, some reports have suggested that various other procedures, such as osteochondral cylinder transplantation or microfracture, may be able to yield equivalent or better results than ACI for cartilage repair in some patients in terms of both histological appearance and clinical outcome.[15,16] The present study was the first to include multilateral results and analyses of reparative tissue after ACI such as his-

tology, quantitative biochemistry, MR imaging, clinical evaluation and arthroscopic assessment; the efficacy of ACI was discussed based upon our results in addition to previous reports by other researchers.

In this study, on histological evaluation at 1 year after ACI, the matrices of reparative tissue stained well with safranin-O and type II collagen antibody. This finding indicated that the reparative tissue qualitatively contained GAG and type II collagen, which are present in native hyaline cartilage. However, on biochemical analysis, the GAG concentration in the reparative tissue matrix was significantly lower than the concentration in native cartilage. These findings, that reparative tissue was inferior to native cartilage, are consistent with those of a previous report.[17] On histological assessment, Richardson et al. reported that in post-ACI reparative tissue the superficial zone of reparative tissue was more fibrocartilaginous with more type I collagen, whereas the deeper zone was predominantly composed of matrix components similar to native cartilage.[6] Additionally, with respect to the distribution of collagen fibers in reparative tissue, Richardson reported that type II collagen was spread throughout the matrix.[6] Thus, our results are consistent with these reports with respect to the qualitative state of reparative tissue at 1 year after ACI: post-ACI reparative tissue contained the same components as normal cartilage. However, the amount and distribution of such components differed from those found in normal cartilage. In particular, reparative tissue contained significantly less GAG than normal cartilage obtained from the same patient.

In contrast, we found that a predominantly viable cell population was observed in reparative tissue. Briggs et al. have reported that transplanted chondrocytes were immature in the phenotype at 1 year after ACI but would probably continue to proliferate and mature.[17] Hence, further long-term follow-up is required to evaluate maturation of the transplanted chondrocytes and biochemical and structural maturation of reparative tissue.

In the current study, the periosteal patch was often likely to be the cause of low scores on histological assessment because of resultant surface irregularity and hypertrophy of periosteum. Brittberg et al. mentioned that the function of the periosteal flap was to close off the defect, to stimulate reproduction of transplanted cultured chondrocytes, and to stimulate the chondrocytes in surrounding native tissue or periosteal cells themselves to enter the defect and repair it.[3] However, recently, the effect of transplanted periosteum has not been consistent among several reports. One group of investigators reported that cells from the cambium layer of the periosteum may possibly be the cell source for repair of cartilage in rabbits.[18] Stimulation of chondrogenesis in periosteum with transforming growth factor[19] and stimulation of the remodeling process in subchondral bone from periosteum have been presented in other reports.[20] In contrast, Henderson et al. reported that any enhancing effect of periosteum on cell proliferation and cell numbers in chondrocyte cultures had not been demonstrated.[21] Several reports even have presented overgrowth of the graft, either in the periosteum or underlying neocartilage, as a major complaint,[3,7,21] along with the need to trim hypertrophic tissue. Nehrer et al. mentioned that early complications after ACI were the result of hypertrophy of the periosteal graft or its inadequate fixation.[8] To prevent these early problems, the use of collagen membrane as a seal instead of periosteum has been suggested.[20] Haddo et al. showed a lower rate of graft hypertrophy in ACI with a collagen membrane than with a periosteal flap.[22] Thus, the use of a periosteal patch might not be the best way to seal the defect during ACI. A collagen membrane may be better to seal the defect to avoid significant postoperative hypertrophy of the graft.

The regeneration of subchondral bone is also an important aspect in regenerating adequate joint components. In this study, more than half of the patients showed normal subchondral bone with the ICRS Visual Histological Assessment Scale. Although in ACI only laboratory-cultivated chondrocytes in suspension are applied to the defect, the effect of such injected cells is not comprehensible. Recent experiments have shown that articular cartilage cells have the potential to form bone tissue.[23] MR imaging after ACI has produced a few reports indicative of reparative subchondral bone in reparative tissue.[5] Normally, osteochondral defects were reported to have refilled with cartilage-like tissue.[12] Qiu et al. suggested that the quality of biological repair of osteochondral defects would be improved if subchondral bone responses were better regulated with proper plate reconstitution, which would more closely approach the level of native tissue.[24] When deep osteochondral defects are treated by conventional ACI, reparative tissues are slow to mature and there are some difficulties in restoring the congruity of articular cartilage.[7] The ACI sandwich technique, which includes cancellous bone grafting to fill the bone defect and periosteal grafting at the level of the subchondral bone plate to prevent bleeding into the cartilage defect, was developed for treatment of such deep osteochondral defects by Peterson.[25] Moreover, tissue engineering of osteochondral composite and special collagen scaffold composites for cartilage and subchondral bone[26] for treatment of osteochondral defects is one possible way to facilitate subchondral bone regeneration and make the operative procedure easier and simpler. In the future, tissue engineering techniques for cartilage[27] along with subchondral bone repair may become the basis for a significant therapeutic option in this field.

With respect to evaluation of reparative cartilage, Roberts et al. reported that there was a significant correlation between MR imaging score and the OsScore (so called because it originated in the Oswestry Laboratory) of samples obtained after ACI.[5] Watanabe et al. reported that the SI index (signal intensity of reparative cartilage divided by the signal intensity of normal cartilage) with 3D-SPGR MR imaging may be a useful parameter for noninvasive evaluation.[28] Furthermore, several sequences have recently been developed, such as delayed gadolinium-enhanced MR imaging for cartilage (dGEMRIC)[29] and T_2 mapping,[30] which can be used to assess cartilage GAG content and collagen arrangement. Because the availability of human biopsy samples after ACI is limited because of the need for invasive techniques to obtain the biopsy, MR imaging seems to be the best tool for morphological assessment of cartilage for long-term follow-up because it can provide detailed information on components noninvasively.

In summary, ACI provided good to excellent clinical outcomes at 1 year with our patients that were consistent with those of several previous reports, even though reparative cartilage varied from hyaline-like cartilage to fibrous cartilage, which is inferior to native cartilage. The biochemical nature of the matrix in reparative tissue was also inferior to that of native cartilage: there was significantly less GAG content in reparative tissue than in normal cartilage at 1 year after ACI. However, the long-term durability of reparative tissue has not yet been reported. Additional long-term, large-scale studies are required to determine the indications, advantages, and limitations of ACI.

References

1. Hunziker EB, Quinn TM, Hauselmann HJ. Quantitative structural organization of normal adult human articular cartilage. Osteoarthritis Cartilage 2002;10:564–72.
2. Mankin HJ. The response of articular cartilage to mechanical injury. J Bone Joint Surg [Am] 1982;64:460–6.
3. Brittberg M, Lindahl A, Nilsson A, Ohlsson C, Isaksson O, Peterson L. Treatment of deep cartilage defects in the knee with autologous chondrocyte transplantation. N Engl J Med 1994; 331:889–95.
4. Peterson L, Brittberg M, Kiviranta I, Akerlund EL, Lindahl A. Autologous chondrocyte transplantation. Biomechanics and long-term durability. Am J Sports Med 2002;30:2–12.
5. Roberts S, McCall IW, Darby AJ, Menage J, Evans H, Harrison PE, et al. Autologous chondrocyte implantation for cartilage repair: monitoring its success by magnetic resonance imaging and histology. Arthritis Res Ther 2003;5:60–73.
6. Richardson JB, Caterson B, Evans EH, Ashton BA, Roberts S. Repair of human articular cartilage after implantation of autologous chondrocytes. J Bone Joint Surg [Br] 1999;81:1064–8.
7. Peterson L, Minas T, Brittberg M, Nilsson A, Sjogren-Jasson E, Lindahl A. Two- to 9-year outcome after autologous chondrocyte transplantation of the knee. Clin Orthop 2000;374:212–34.
8. Nehrer S, Spetor M, Minas T. Histologic analysis of tissue after failed cartilage repair procedures. Clin Orthop 1999;365:149–62.
9. ICRS Cartilage Injury Evaluation Package. http://www.cartilage.org/_files/contentmanagement/ICRS_evaluation.pdf
10. Mainil-Varlet P, Aigner T, Brittberg M, Bullough P, Hollander A, Hunziker E, et al. Histological assessment of cartilage repair: a report by the histology endpoint committee of the International Cartilage Repair Society (ICRS). J Bone Joint Surg [Am] 2003; 85:45–57.
11. Shinmei M, Miyauchi S, Machida A, Miyazaki K. Quantitation of chondroitin 4-sulfate and chondroitin 6-sulfate in pathologic joint fluid. Arthritis Rheum 1992;35:1304–8.
12. Disler DG. Fat-suppressed three-dimensional spoiled gradient-recalled MR imaging: assessment of articular and physeal hyaline cartilage. AJR Am J Roentgenol 1997;169:1117–23.
13. Henderson IJP, Tuy B, Connell D, Oakes B, Hettwer WH. Prospective clinical study of autologous chondrocyte implantation and correlation with MRI at three and 12 months. J Bone Joint Surg [Br] 2003;85:1060–6.
14. Lysholm J, Gillquist J. Evaluation of knee ligament surgery results with special emphasis on use of a scoring scale. Am J Sports Med 1982;10:150–4.
15. Horas U, Pelinkovic D, Herr G, Aigner T, Schnettler R. Autologous chondrocyte implantation and osteochondral cylinder transplantation in cartilage repair of the knee joint: a prospective, comparative trial. J Bone Joint Surg [Am] 2003;85:185–92.
16. Knutsen G, Engebretsen L, Ludvigsen TC, Drogset JO, Grøntvedt T, Solheim E, et al. Autologous chondrocyte implantation compared with microfracture in the knee. A randomized trial. J Bone Joint Surg [Am] 2004;86:455–64.
17. Briggs TWR, Mahroof S, David LA, Flannelly J, Pringle J, Bayliss M. Histological evaluation of chondral defects after autologous chondrocyte implantation of the knee. J Bone Joint Surg [Br] 2003;85:1077–83.
18. Zarnett R, Delaney JP, Driscoll SW, Salter RB. Cellular origin and evolution of neochondrogenesis in major full-thickness defects of a joint surface treated by free autogenous periosteal grafts and subjected to continuous passive motion in rabbits. Clin Orthop 1987;222:267–74.
19. O'Driscoll SW, Recklies AD, Poole AR. Chondrogenesis in periosteal explants. An organ culture model for in vitro study. J Bone Joint Surg [Am] 1994;76:1042–51.
20. Russlies M, Behrens P, Ehlers EM, Brohl C, Vindigni C, Spector M, et al. Periosteum stimulates subchondral bone densification in autologous chondrocyte transplantation in a sheep model. Cell Tissue Res 2005;319:133–42.
21. Henderson I, Tuy B, Oakes B. Reoperation after autologous chondrocyte implantation. Indications and findings. J Bone Joint Surg [Br] 2004;86:205–11.
22. Haddo O, Mahroof S, Higgs D, David L, Pringle J, Bayliss M, et al. The use of chondrogide membrane in autologous chondrocyte implantation. Knee 2004;11:51–5.
23. Tallheden T, Dennis JE, Lennon DP, Sjögren-Janson E, Caplan AI, Lindahl A. Phenotypic plasticity of human articular chondrocytes. J Bone Joint Surg [Am] 2003;85(suppl 2):93–100.
24. Qui YS, Shahgaldi BF, Revell WJ, Heatley FW. Observations of subchondral plate advancement during osteochondral repair: a histomorphometric and mechanical study in the rabbit femoral condyle. Osteoarthritis Cartilage 2003;11:810–20.
25. Peterson L. Chondrocyte transplantation. In: Jackson DW, editor. Master techniques in orthopaedic surgery: reconstructive knee surgery. Philadelphia: Lippincott Williams & Wilkins; 2003. p. 353–73.
26. Schaefer D, Martin I, Jundt G, Seidel J, Heberer M, Grodzinsky A, et al. Tissue-engineered composites for the repair of large osteochondral defects. Arthritis Rheum 2002;46:2524–34.
27. Marcacci M, Berruto M, Brocchetta D, Delcogliano A, Ghinelli D, Gobbi A, et al. Articular cartilage engineering with Hyalograft C: 3-year clinical results. Clin Orthop 2005;435:96–105.

28. Watanabe A, Wada Y, Obata T, Sasho T, Ueda T, Tamura M, et al. Time course evaluation of reparative cartilage with MR imaging after autologous chondrocyte implantation. Cell Transplant 2005;14:695–700.
29. Bashir A, Gray ML, Boutin RD, Burstein D. Glycosaminoglycan in articular cartilage: in vivo assessment with delayed Gd(DTPA) (2-)-enhanced MR imaging. Radiology 1997;205:551–8.
30. Mosher TJ, Smith H, Dardzinski BJ, Schmithorst VJ, Smith MB. MR imaging and T_2 mapping of femoral cartilage: in vivo determination of the magic angle effect. AJR Am J Roentgenol 2001; 177:665–9.

J Nutr Sci Vitaminol, 53, 191–197, 2007

Effects of Alfacalcidol on Cancellous and Cortical Bone Mass in Rats Treated with Glucocorticoid: A Bone Histomorphometry Study

Jun IWAMOTO[1], Azusa SEKI[2], Tsuyoshi TAKEDA[1], Harumoto YAMADA[3], Yoshihiro SATO[4] and James K. YEH[5]

[1]*Department of Sports Medicine, Keio University School of Medicine, Shinjuku-ku, Tokyo 160–8582, Japan*
[2]*Hamri Co., Ltd., Tokyo, Japan*
[3]*Department of Orthopaedic Surgery, Fujita Health University, Aichi, Japan*
[4]*Department of Neurology, Mitate Hospital, Fukuoka, Japan*
[5]*Metabolism Laboratory, Department of Medicine, Winthrop-University Hospital, NY, USA*

(Received November 9, 2006)

Summary The beneficial effects of alfacalcidol (ALF) on bone mass, bone formation, and bone resorption have been established in ovariectomized rats. Our previous studies showed that high-dose glucocorticoid (GC) administration (methylprednisolone sodium succinate, 5.0 mg/kg, s.c., 3 times a week) for 4 wk induced cancellous osteopenia without significantly affecting cortical bone mass in Sprague-Dawley rats, and that high-dose GC administration for 8 wk also resulted in cortical osteopenia. The purpose of the present study was to examine the effects of ALF on cancellous and cortical bone mass in GC-treated rats. Forty female Sprague-Dawley rats, 3 mo of age, were randomized by the stratified weight method into four groups of 10 rats each, as follows: age-matched control group (CON); 8-wk GC administration with administration of vehicle during the latter 4 wk of treatment (GC group); 8-wk GC administration with administration of a low dose of ALF (0.08 μg/kg) during the latter 4 wk of treatment (low-dose ALF group); 8-wk administration of GC with administration of a high dose of ALF (0.16 μg/kg) during the latter 4 wk of treatment (high-dose ALF group). The GC (methylprednisolone sodium succinate, 5.0 mg/kg) was administered subcutaneously 3 times a week, and ALF was administered orally 5 times a week. At the end of the experiment, static and dynamic bone histomorphometric analyses were performed on cancellous bone of the proximal tibial metaphysis and cortical bone of the tibial diaphysis. Eight-week GC administration resulted in loss of the cancellous bone volume/total tissue volume (BV/TV) and percent cortical area (Ct Ar) as a result of decreased trabecular bone formation, increased trabecular and endocortical bone resorption, and decreased periosteal bone formation. Low-dose ALF restored the cancellous BV/TV by mildly suppressing bone resorption and restoring bone formation, whereas high-dose ALF increased it beyond the value observed in the age-matched controls by strongly suppressing bone resorption and markedly increasing bone formation. Both low- and high-dose ALF prevented the GC-induced reduction of the percent Ct Ar by increasing periosteal bone formation and suppressing endocortical bone resorption. The effects of ALF on cancellous bone mass, bone formation, and bone resorption were all dose-dependent. The present study showed the beneficial effects of ALF on cancellous and cortical bone mass in GC-treated rats.

Key Words glucocorticoid, osteopenia, vitamin D_3, alfacalcidol, rat

Alfacalcidol (ALF) is widely used for the treatment of osteoporosis in postmenopausal women in Japan. Clinical studies have shown that ALF reduces bone turnover, maintains or slightly increases the lumbar bone mineral density (BMD), and reduces the incidence of vertebral fractures in postmenopausal women with osteoporosis (*1*, *2*). A preclinical study has also shown that ALF prevents cancellous bone loss and increases cortical bone mass by suppressing bone resorption and maintaining or even increasing bone formation in ovariectomized rats (*3*). Thus, the beneficial effects of ALF on bone mass and bone metabolism in ovariectomized rats, as well as on the incidence of vertebral fractures has been demonstrated in postmenopausal women with osteoporosis.

Not only postmenopausal osteoporosis, but also glucocorticoid (GC)-induced osteoporosis is a serious health threat, because GC treatment rapidly induces bone loss and deterioration of bone quality, leading to an increased risk of fractures. Very few studies have reported on the efficacy of ALF for GC-induced osteoporosis in Japan. Meta-analyses and a systematic review in western countries have revealed the efficacy of ALF for maintaining the lumbar BMD and reducing the incidence of vertebral fractures in patients with GC-induced osteoporosis (*4–6*). A randomized controlled

E-mail: jiwamoto@sc.itc.keio.ac.jp

trial showed the effect of ALF on bone metabolism in patients who were on GC treatment; ALF reduced the severity of hyperparathyroidism and stimulated bone formation (*7*). However, the effect of ALF on cancellous and cortical bone mass, as well as on bone formation and bone resorption has not necessarily been established in GC-treated patients.

Our previous studies revealed that high-dose GC administration (methylprednisolone sodium succinate, 5.0 mg/kg, s.c., 3 times a week) for 4 wk induced cancellous osteopenia without significantly affecting cortical bone mass in Sprague-Dawley rats, and that high-dose GC administration for 8 wk also induced cortical osteopenia (*8*, *9*) (a part of the data is not shown). These results lend support to evidence suggesting that GC-induced osteoporosis is more evident in cancellous than in cortical bone (*10*). We also demonstrated the preventive and therapeutic effects of calcitriol, the active and hormonal form of vitamin D that plays a central role in bone mineral homeostasis, on cancellous and cortical bone loss in GC-treated rats (*8*, *9*); calcitriol suppressed bone resorption and maintained or even increased bone formation, thereby attenuating the GC-induced cancellous bone loss and increasing cancellous bone mass in rats with GC-induced osteopenia. However, the effect of calcitriol on cortical bone in GC-treated rats remains uncertain.

Recently, a few preclinical studies have reported the skeletal efficacy of ALF, the prodrug of calcitriol, in GC-treated animals. ALF suppressed bone resorption and maintained bone formation, but failed to maintain the growth-dependent increase of cancellous bone mass and structure in young growing minipigs (*11*). However, very few preclinical studies have reported the skeletal effects of ALF in GC-treated rats. Thus, the purpose of the present study was to clarify the effects of ALF on both cancellous and cortical bone mass using an animal model of GC-induced osteoporosis, the GC-treated rat, and to determine whether ALF would exert the same effects on cancellous and cortical bone in the GC-treated rats as in ovariectomized rats.

MATERIALS AND METHODS

Treatment of animals. Forty female Sprague-Dawley rats, 3 mo of age, were purchased from Hilltop Lab. Animals, Inc. (Scottdale, PA, USA). The animals were housed under local vivarium conditions (temperature 23.8°C and 12-h on/off light cycle), fed a pelleted standard chow diet containing 1.36% calcium and 2,400 IU/kg of vitamin D (Rodent Diet 8604, Harlan Teklad, Madison, WI, USA), and had free access to water. Following a 1-wk adaptation period to the new environment, the rats were randomized by the stratified weight method into four groups of 10 rats each, as follows: age-matched control (CON group), 8 wk GC administration with administration of vehicle during the latter 4 wk of treatment (GC alone group), 8-wk GC administration with administration of a low dose of alfacalcidol (0.08 μg/kg body weight) during the latter 4 wk of treatment (low-dose ALF group), and 8-wk GC administration with administration of a high dose of alfacalcidol (0.16 μg/kg body weight) during the latter 4 wk of treatment (high-dose ALF group). Methylprednisolone sodium succinate (Pharmacia & Upjohn Company, Kalamazoo, MI, USA) was administered as the GC, at the dose of 5.0 mg/kg body weight 3 times a week by subcutaneous injection. ALF (Teijin Pharma, Tokyo, Japan) was dissolved in 0.1 mL of PBS containing 0.25% ethanol and 0.1% Tween 20, and administered by gavage deep into the mouth at the dose of 0.08 or 0.16 μg/kg body weight, depending on the group, 5 times a week. This dose of ALF is considered to be an effective dose in rats, in accordance with previously published data (*3*). The body weight of the rats was monitored weekly, and the total experimental period was 8 wk. The study was carried out at Winthrop-University Hospital, and the animals were maintained according to the National Institutes of Health (NIH) Guidelines for the Care and Use of Laboratory Animals. All the animal experimental protocols were approved by the Laboratory Animal Care Committee of Winthrop-University Hospital.

Preparation of specimens. All the rats were labeled with 10 mg/kg of calcein (Sigma Chemical, St. Louis, MO, USA) injected intramuscularly 11 d and 4 d before they were sacrificed. The animals were anesthetized by ketamine injected intraperitoneally at the dose of 80 mg/kg, together with xylazine at the dose of 12 mg/kg, and sacrificed by exsanguination. A blood specimen, the right femur, and the right tibia were collected from every animal.

After separation of the serum, the serum samples were stored at −20°C, and then used for measurements of the serum creatinine and serum calcium levels in automated equipment (Dada Behring Model RXL, Bakersfield, CA, USA). The femurs were stored at −20°C, and then used for measurements of the bone mineral content (BMC) and BMD by dual-energy X-ray absorptiometry (DXA) using a Hologic QDR-2000 plus (Hologic Inc., Bedford, MA, USA). The coefficient of variation of the femoral BMC and BMD measurements at our laboratory was less than 1.0% (*12*). The tibiae were used for bone histomorphometric analysis; the bones were fixed overnight in 40% cold ethanol, and then cut into three parts using an Isomet saw (Buehler, Lake Bluff, IL, USA). The proximal tibial metaphysis and tibial diaphysis were stained with Villanueva Osteochrome Bone Stain (Polyscience, Warrington, PA, USA) for 5 d. The specimens were then dehydrated sequentially in ascending concentrations of ethanol (70, 95, and 100%) and xylene and then embedded in methyl methacrylate (EM Science, Gibbstown, NJ, USA) at 4°C, in accordance with the method described by Erben (*13*). Cross-sections of the tibial diaphysis just proximal to the tibio-fibular junction were cut at 40-μm thickness using a diamond wire Histo-Saw machine (Delaware Diamond Knives, Wilmington, DE, USA), and the thickness of each cross-sectional specimen was determined with an Inspectors' Dial Bench Gauge (L.S. Starrett, Athol, MA, USA). Frontal sections of the proximal tibial

metaphysis were cut at 5-μm thickness using a microtome (Leica RM2155; Leica Inc., Nussloch, Germany), transferred onto chromium-gelatin-coated slides, dried overnight under pressure at 42°C, and then coverslipped with Eukitt mounting medium (Calibrated Instruments, Hawthorne, NY, USA) for static and dynamic histomorphometric analyses.

Bone histomorphometric analysis of the tibia. A digitizing morphometric system was used to measure the bone histomorphometric parameters. The system consisted of an epifluorescence microscope (Nikon E-400, OsteoMetrics, Atlanta, GA, USA), an Osteomeasure High Resolution Color Subsystem (OsteoMetrics) coupled to an IBM computer, and a morphometry program (OsteoMetrics). The measured parameters for cancellous bone included the total tissue volume (TV), bone volume (BV), bone surface (BS), eroded surface (ES), single- and double-labeled surface (sLS and dLS, respectively), and the interlabel width. These data were used to calculate the cancellous bone volume (BV/TV), trabecular number (Tb N), trabecular thickness (Tb Th), trabecular separation (Tb Sp), ES/BS, mineralizing surface (MS)/BS [(sLS/2+dLS)/BS], mineral apposition rate (MAR), bone formation rate (BFR)/BS, and BFR/BV, in accordance with the standard nomenclature proposed by Parfitt et al. (*14*). In the present study, the region of the cancellous bone marked for the measurements was 1–4 mm distal to the lower margin of the growth plate in the proximal tibial metaphysis, which consists of secondary spongiosa. The following parameters of cortical bone were measured: the total tissue area (Tt Ar) and cortical bone area (Ct Ar), the periosteal and endocortical BS (perimeter), sLS, dLS, interlabel width, and the endocortical ES. These data were used to calculate the marrow area (Ma Ar), percent Ct Ar, and percent Ma Ar, as well as the periosteal and endocortical MS/BS [(sLS/2+dLS)/BS], MAR and BFR/BS, and endocortical ES/BS

Statistical analysis. All the data were expressed as means±standard deviation (SD). Data comparisons between the CON group and the GC alone, low-dose ALF, and high-dose ALF groups were performed by analysis of variance (ANOVA) with Dunnett's test. Data comparisons among the GC alone, low-dose ALF, and high-dose ALF groups were performed by ANOVA with the Tukey-Kramer test. All statistical analyses were performed using the Stat View J-5.0 program on a Macintosh computer. A significance level of $p<0.05$ was set for all the comparisons.

RESULTS

Body weight, femoral length, BMC and BMD, and serum creatinine and calcium levels (Table 1)

The GC group and the low-dose and high-dose ALF groups showed a lower body weight as compared with that of the age-matched controls.

In the GC group, while no significant change of the femoral length was noted, the femoral BMC and BMD were decreased. The low-dose ALF group showed no significant differences in the femoral BMC and BMD as compared with the values in the age-matched controls, and the high-dose ALF group showed no significant difference in the femoral BMC, but a higher femoral BMD as compared with the values in the age-matched controls.

No significant changes in the serum creatinine or calcium levels were observed in the GC group. However, the serum calcium levels were increased in both the low-dose and high-dose ALF groups, with the increase being more pronounced in the high-dose ALF group than in the low-dose ALF group. On the other hand, there were no significant changes in the serum creatinine level in either the low-dose or the high-dose ALF group, suggesting the safety of ALF from the point of view of kidney functions.

Histomorphometric analysis of cancellous bone of the proximal tibial metaphysis (Fig. 1 and Table 2)

A decrease of the cancellous BV/TV, Tb Th, and Tb N, and increase of the Tb Sp were observed in the GC group as a result of decreased bone formation (MAR) and increased bone resorption (ES/BS). The cancellous BV/TV was restored, reduction in Tb Th was attenuated,

Table 1. Body weight, femoral length, BMC, BMD, and serum creatinine and calcium levels.

	Initial body weight (g)	Final body weight (g)	Femoral length (mm)	Femoral BMC (mg)	Femoral BMD (mg/cm^2)	Serum creatinine (mg/dL)	Serum calcium (mg/dL)
CON	288±6	308±17	35.6±0.4	508±24	272±7	0.57±0.08	9.9±0.2
GC	286±6	290±16[a]	35.4±0.5	472±33[a]	260±8[a]	0.59±0.07	9.7±0.3
Low-dose ALF	292±8	289±11[a]	35.6±0.3	519±18[b]	277±6[b]	0.60±0.07	10.5±0.5[ab]
High-dose ALF	290±7	276±9[ab]	35.7±0.4	524±20[b]	281±6[ab]	0.63±0.12	11.4±0.4[abc]

Data are expressed as mean±SD. Data comparisons between the CON group and the GC, low-dose ALF, and high-dose ALF groups were performed by analysis of variance (ANOVA) with the Dunnett's test. Data comparisons among the GC, low-dose ALF, and high-dose ALF groups were performed by ANOVA with the Tukey-Kramer test.
GC: glucocorticoid, ALF: alfacalcidol, BMC: bone mineral content, BMD: bone mineral density.
[a] Significant vs. CON; [b] significant vs. GC; [c] significant vs. Low-dose ALF.
CON: age-matched control, 8GC: 8-wk GC administration, Low-dose ALF: 4-wk GC administration followed by 4-wk GC and low-dose ALF administration, High-dose ALF: 4-wk GC administration followed by 4-wk GC and high-dose ALF administration.

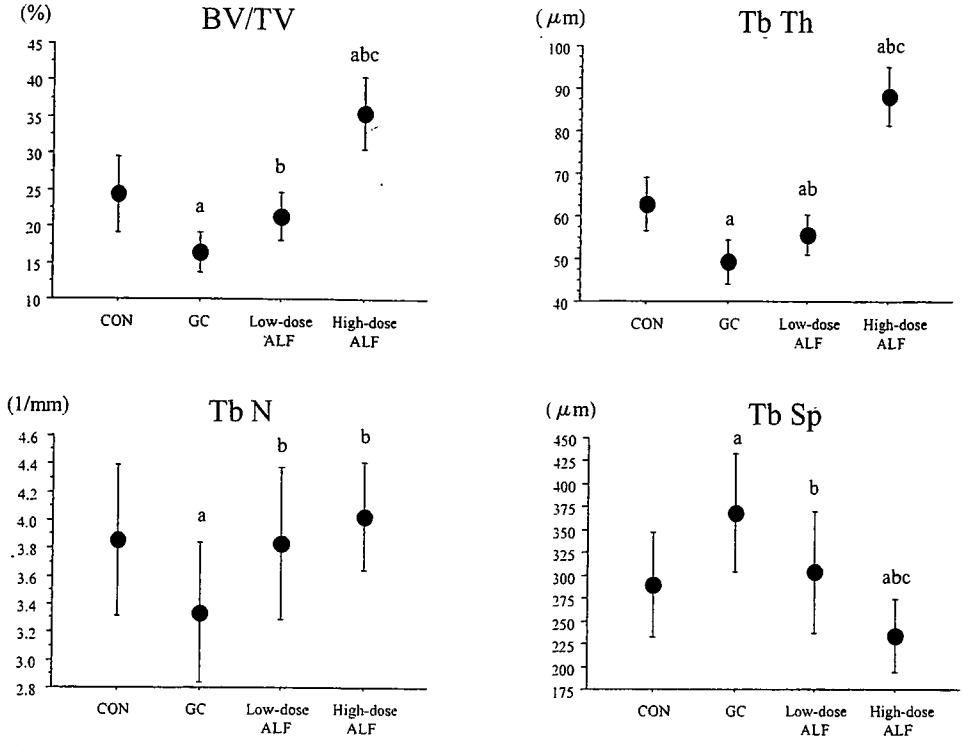

Fig. 1. Bone histomorphometric analysis of cancellous bone of the proximal tibial metaphysis—Structural parameters. Data are expressed as mean±SD. Data comparisons between the CON group and the GC, low-dose ALF, and high-dose ALF groups were performed by analysis of variance (ANOVA) with the Dunnett's test. Data comparisons among the GC, low-dose ALF, and high-dose ALF groups were performed by ANOVA with the Tukey-Kramer test. GC: glucocorticoid, ALF: alfacalcidol, BV: bone volume, TV: total tissue volume, Tb Th: trabecular thickness, Tb N: trabecular number, Tb Sp: trabecular separation. [a] Significant vs. CON; [b] significant vs. GC; [c] significant vs. Low-dose ALF. CON: age-matched control, 8GC: 8-wk GC administration, Low-dose ALF: 4-wk GC administration followed by 4-wk GC and low-dose ALF administration, High-dose ALF: 4-wk GC administration followed by 4-wk GC and high-dose ALF administration.

Table 2. Bone histomorphometric analysis of cancellous bone of the proximal tibial metaphysis—Formative and resorptive parameters.

	MS/BS (%)	MAR (μm/d)	BFR/BS (μm³/μm²/d)	BFR/BV (%/y)	ES/BS (%)
CON	9.0±2.9	1.22±0.12	14.7±6.8	143±65	3.7±1.7
GC	11.2±4.3	0.93±0.16[a]	11.2±4.2	142±58	12.1±5.4[a]
Low-dose ALF	11.1±3.5	1.11±0.29[b]	12.1±4.2	133±48	7.2±2.2[ab]
High-dose ALF	22.5±3.6[abc]	1.35±0.12[abc]	30.3±5.0[abc]	210±30[abc]	0.6±1.1[abc]

Data are expressed as mean±SD. Data comparisons between the CON group and the GC, low-dose ALF, and high-dose ALF groups were performed by analysis of variance (ANOVA) with the Dunnett's test. Data comparisons among the GC, low-dose ALF, and high-dose ALF groups were performed by ANOVA with the Tukey-Kramer test.
GC: glucocorticoid, ALF: alfacalcidol, MS: mineralizing surface, BS: bone surface, MAR: mineral apposition rate, BFR: bone formation rate, BV: bone volume, ES: eroded surface.
[a] Significant vs. CON; [b] significant vs. GC; [c] significant vs. Low-dose ALF.
CON: age-matched control, 8GC: 8-wk GC administration, Low-dose ALF: 4-wk GC administration followed by 4-wk GC and low-dose ALF administration, High-dose ALF: 4-wk GC administration followed by 4-wk GC and high-dose ALF administration.

reduction in Tb N was prevented and the Tb Sp was decreased in the low-dose ALF group, as a result of prevention of the GC-induced reduction of bone formation (MAR) and mild suppression of bone resorption (ES/BS). In the high-dose ALF group, the cancellous BV/TV and Tb Th were markedly increased, reduction in Tb N was prevented, and the Tb Sp was markedly decreased as a result of the markedly decreased bone resorption (ES/BS) and markedly increased bone formation (MS/BS, MAR, BFR/BS, BFR/BV). The effects of ALF on the cancellous BV/TV, bone formation, and bone resorption were all dose-dependent.

Histomorphometric analysis of cortical bone of the tibial diaphysis (Fig. 2 and Table 3)

The percent Ct Ar was decreased and the percent Ma Ar increased in the GC group, as a result of decreased

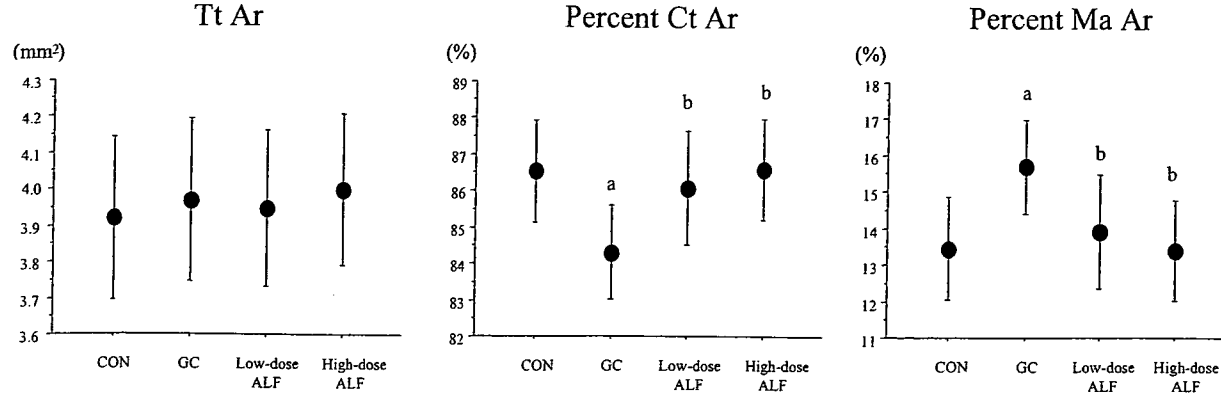

Fig. 2. Bone histomorphometric analysis of cortical bone of the tibial diaphysis—Structural parameters. Data are expressed as mean±SD. Data comparisons between the CON group and the GC, low-dose ALF, and high-dose ALF groups were performed by analysis of variance (ANOVA) with the Dunnett's test. Data comparisons among the GC, low-dose ALF, and high-dose ALF groups were performed by ANOVA with the Tukey-Kramer test. GC: glucocorticoid, ALF: alfacalcidol, Tt Ar: total tissue area, Ct Ar: cortical area, Ma Ar: marrow area. [a] Significant vs. CON; [b] significant vs. GC; [c] significant vs. Low-dose ALF. CON: age-matched control, 8GC: 8-wk GC administration, Low-dose ALF: 4-wk GC administration followed by 4-wk GC and low-dose ALF administration, High-dose ALF: 4-wk GC administration followed by 4-wk GC and high-dose ALF administration.

Table 3. Bone histomorphometric analysis of cortical bone of the tibial diaphysis—Formative and resorptive parameters.

	Periosteal			Endocortical			
	MS/BS (%)	MAR (μm/d)	BFR/BS (μm³/μm²/d)	MS/BS (%)	MAR (μm/d)	BFR/BS (μm³/μm²/d)	ES/BS (%)
CON	23.2±4.1	0.92±0.09	21.3±5.1	0.6±1.6	0.09±0.27	0.45±1.42	6.7±2.1
GC	17.8±5.2[a]	0.86±0.14	15.6±6.2[a]	1.6±2.0	0.27±0.44	1.18±1.93	10.4±2.1[a]
Low-dose ALF	36.0±6.0[a]	1.02±0.21	36.5±8.2[ab]	4.1±8.7	0.20±0.41	3.62±9.09	5.5±1.1[b]
High-dose ALF	37.1±11.5[a]	1.20±0.17[ab]	43.5±11.1[ab]	0.6±1.0	0.00±0.00	0.00±0.00	6.9±1.7[b]

Data are expressed as mean±SD. Data comparisons between the CON group and the GC, low-dose ALF, and high-dose ALF groups were performed by analysis of variance (ANOVA) with the Dunnett's test. Data comparisons among the GC, low-dose ALF, and high-dose ALF groups were performed by ANOVA with the Tukey-Kramer test.
GC: glucocorticoid, ALF: alfacalcidol, MS: mineralizing surface, BS: bone surface, MAR: mineral apposition rate, BFR: bone formation rate, ES: eroded surface.
[a] Significant vs. CON; [b] significant vs. GC; [c] significant vs. Low-dose ALF.
CON: age-matched control, 8GC: 8-wk GC administration, Low-dose ALF: 4-wk GC administration followed by 4-wk GC and low-dose ALF administration. High-dose ALF: 4-wk GC administration followed by 4-wk GC and high-dose ALF administration.

periosteal bone formation (MS/BS, BFR/BS) and increased endocortical bone resorption (ES/BS). The reduction in the percent Ct Ar and increase in the percent Ma Ar were both prevented in both the low-dose and high-dose ALF groups, as a result of increased periosteal bone formation (BFR/BS) and suppressed endocortical bone resorption (ES/BS).

DISCUSSION

The beneficial effects of ALF on cancellous and cortical bone mass have already been established in ovariectomzied rats (*3*). The present study was conducted to clarify the effects of ALF on cancellous and cortical bone mass in GC-treated rats, and to determine whether ALF would exert the same effects on cancellous and cortical bone in the GC-treated rats as in ovariectomized rats. ALF treatment was started after GC had been administered for 4 wk, and continued for 4 wk to determine the therapeutic effect of ALF on the GC-induced cancellous osteopenia and its preventive effect against cortical osteopenia in GC-treated rats. The cancellous BV/TV was restored in the low-dose ALF group, and even increased in the high-dose ALF group, and the GC-induced reduction of the Ct Ar was prevented in both the groups. The effect of ALF on the cancellous bone mass was found to be dose-dependent. The present study thus showed the beneficial effects of ALF on cancellous and cortical bone mass in GC-treated rats.

GC administration has been shown to induce loss of the cancellous BV/TV, Tb N, and Tb Th of the lumbar spine in rats and also loss of the three-dimensional cancellous BV/TV and Tb Th, an increase in the trabecular bone pattern factor in the lumbar spine of minipigs (*15–21*). GC-induced cancellous osteopenia has been shown to be associated with decreased bone formation and increased bone resorption, and the key histological

feature of corticosteroid-induced cancellous bone loss has been reported to be the reduction in the Tb Th, reflecting suppressed bone formation (*22*). In the present study, GC administration for 8 wk was shown to be associated with a decrease of the cancellous BV/TV, Tb Th and Tb N, and increase of the Tb Sp as a result of decreased bone formation and increased bone resorption.

The beneficial effects of ALF on cancellous bone mass and structure in ovariectomized rats has been well documented; ALF increased not only cancellous bone mass and the Tb Th, but also three-dimensional cancellous bone mass by reinforcing the interconnectivities and structures of the trabeculae (*3*, *23*). The beneficial effect of ALF on cancellous bone mass in ovariectomized rats was primarily due to its suppression of bone resorption and maintenance or even stimulation of bone formation (*3*). In the present study, low-dose ALF restored the loss of the cancellous BV/TV, attenuated the reduction in the Tb Th, prevented the reduction in the Tb N and decreased the Tb Sp in the GC-treated rats, and high-dose ALF markedly increased the cancellous BV/TV and Tb Th, prevented the reduction in the Tb N, and markedly decreased the Tb Sp in the GC-treated rats. The main skeletal effect of ALF in the GC-treated rats was considered to be suppression of bone resorption and maintenance or even stimulation of bone formation, which might be similar to its actions in ovariectomized rats, despite the different influence of ovariectomy and GC administration on bone formation. The effects of ALF on cancellous bone mass and structure, and bone formation and resorption were all dose-dependent. Thus, the present study demonstrated the beneficial effects of ALF on cancellous bone mass and metabolism in GC-treated rats, which appeared to be similar to the vitamin's effects in ovariectomized rats.

It has been reported that GC administration induces cortical osteopenia in rats as a result of decreased periosteal and/or endocortical bone formation and increased endocortical bone resorption (*15–17*). In the present study, GC administration for 8 wk decreased the percent Ct Ar and increased the percent Ma Ar as a result of decreased periosteal bone formation and increased endocortical bone resorption.

The beneficial effects of ALF on cortical bone mass in ovariectomized rats has been documented; ALF treatment increased cortical bone mass as a result of increased endocortical bone formation and decreased endocortical bone resorption (*3*). In the present study, both the low- and high-dose ALF prevented the reduction of the percent Ct Ar and increase of the percent Ma Ar in the GC-treated rats as a result of increased periosteal bone formation and suppressed endocortical bone resorption. The primary effect of ALF on endocortical bone metabolism might be similar in both ovariectomized and GC-treated rats. We showed the effects of ALF on periosteal bone formation in the GC-treated rats. However, the actions of ALF seem to be less potent on cortical bone than on cancellous bone.

We measured the femoral BMC and BMD to determine the effect of ALF on the bone histomorphometric parameters. GC administration decreased both the femoral BMC and BMD, consistent with the alterations of cancellous and cortical bone mass as evaluated by histomorphometric analyses. Both low- and high-dose ALF improved the femoral BMC and BMD, and the effect of ALF on the femoral BMD was dose-dependent. The effect of ALF on the femoral BMD and BMC was consistent with its effect on the cancellous BV/TV and percent Ct Ar, respectively. Thus, the beneficial effects of ALF on cancellous and cortical bone mass were suggested by its observed effects on the femoral BMD and BMC.

Thus, we showed the beneficial effects of ALF on cancellous and cortical bone mass in GC-treated rats. In this context, the effect of a synthetic vitamin D analog, ED-71, which is not yet commercially available for the treatment of osteoporosis in Japan, on cancellous and cortical bone was reported in young growing GC-treated rats in a previous study (*17*); ED-71 increased the BMD, cancellous BV/TV and Tb Th, and also the mechanical strength of the lumbar vertebral body in a dose-dependent manner, as compared with the changes observed in a non-treated group, and attenuated the GC-induced reductions in the femoral BMD and mechanical bone strength; these effects of ED-71 were attributed to suppressed bone resorption and increased mineralization. However, the actions of ED-71 also appeared to be less potent on the cortical bone. The overall effects of ALF and ED-71 on the cancellous and cortical bone mass and bone metabolism appeared to be similar.

Both low- and high-dose ALF increased the serum calcium level, with the effect of high-dose ALF being more pronounced than that of low-dose ALF. ALF has also been reported to increase the serum calcium levels in ovariectomized rats (*3*). Thus, the risk of hypercalcemia should be taken into consideration when selecting to use ALF for treatment. On the other hand, the serum creatinine level was not affected by ALF, suggesting its safety from the point of view of kidney functions.

In conclusion, the present study showed that ALF was efficacious for preventing cancellous bone loss, even increasing cancellous bone mass, and increasing cortical bone mass induced by GC in GC-treated rats. However, at effective doses, ALF also induced elevation of the serum calcium levels. The effects of ALF on cancellous bone mass, bone formation, bone resorption and the serum calcium levels were all dose-dependent. The effect of ALF on cancellous bone mass and metabolism was similar in ovariectomized and GC-treated rats.

REFERENCES

1) Orimo H, Shiraki M, Hayashi Y, Hoshino T, Onaya T, Miyazaki S, Kurosawa H, Nakamura T, Ogawa N. 1994. Effects of 1 alpha-hydroxyvitamin D_3 on lumbar bone mineral density and vertebral fractures in patients with postmenopausal osteoporosis. *Calcif Tissue Int* **54**: 370–376.

2) Shiraki M, Fukuchi M, Kiriyama T, Okamoto S, Ueno T, Sakamoto H, Nagai T. 2004. Alfacalcidol reduces accel-

erated bone turnover in elderly women with osteoporosis. *J Bone Miner Metab* **22**: 352–359.

3) Shiraishi A, Takeda S, Masaki T, Higuchi Y, Uchiyama Y, Kubodera N, Sato K, Ikeda K, Nakamura T, Matsumoto T, Ogata E. 2000. Alfacalcidol inhibits bone resorption and stimulate formation in an ovariectomized rat model of osteoporosis: distinct actions from estrogen. *J Bone Miner Res* **15**: 770–779.

4) de Nijs RN, Jacobs JW, Algra A, Lems WF, Bijlsma JW. 2004. Prevention and treatment of glucocorticoid-induced osteoporosis with active vitamin D_3 analogues: a review with meta-analysis of randomized controlled trials including organ transplantation studies. *Osteoporos Int* **15**: 589–602.

5) Richy F, Ethgen O, Bruyere O, Reginster JY. 2004. Efficacy of alphacalcidol and calcitriol in primary and corticosteroid-induced osteoporosis: a meta-analysis of their effects on bone mineral density and fracture rate. *Osteoporos Int* **15**: 301–310.

6) Richy F, Schacht E, Bruyere O, Ethgen O, Gourlay M, Reginster JY. 2005. Vitamin D analogs versus native vitamin D in preventing bone loss and osteoporosis-related fractures: a comparative meta-analysis. *Calcif Tissue Int* **76**: 176–186.

7) Lakatos P, Nagy Z, Kiss L, Horvath C, Takacs I, Foldes J, Speer G, Bossanyi A. 2000. Prevention of corticosteroid-induced osteoporosis by alfacalcidol. *Z Rheumatol* **59** (Suppl 1): 48–52.

8) Iwamoto J, Seki A, Takeda T, Sato Y, Yamada H, Shen CL, Yeh JK. 2006. Preventive effects of risedronate and calcitriol on cancellous osteopenia in rats treated with high-dose glucocorticoid. *Exp Anim* **55**: 349–355.

9) Iwamoto J, Seki A, Takeda T, Sato Y, Yamada H, Shen CL, Yeh JK. 2006. Comparative effects of risedronate and calcitriol on cancellous bone in rats with glucocorticoid-induced osteopenia. *J Nutr Sci Vitaminol* **52**: 21–27.

10) van Staa TP, Leufkens HG, Abenhaim L, Zhang B, Cooper C. 2000. Use of oral corticosteroids and risk of fractures. *J Bone Miner Res* **15**: 993–1000.

11) Akahoshi S, Sakai A, Arita S, Ikeda S, Morishita Y, Tsutsumi H, Ito M, Shiraishi A, Nakamura T. 2005. Modulation of bone turnover by alfacalcidol and/or alendronate does not prevent glucocorticoid-induced osteoporosis in growing minipigs. *J Bone Miner Metab* **23**: 341–350.

12) Prakasam G, Yeh JK, Chen MM, Castro-Magana M, Liang CT, Aloia JF. 1999. Effects of growth hormone and testosterone on cortical bone formation and bone density in aged orchiectomized rats. *Bone* **24**: 491–497.

13) Erben RG. 1997. Embedding of bone samples in methylmethacrylate: an improved method suitable for bone histomorphometry, histochemistry, and immunohistochemistry. *J Histochem Cytochem* **45**: 307–313.

14) Parfitt AM, Drezner MK, Glorieux FH, Kanis JA, Malluche H, Meunier PJ, Ott SM, Recker RR. 1987. Bone histomorphometry: standardization of nomenclature, symbols, and units. Report of the ASMBR Histomorphometry Nomenclature Committee. *J Bone Miner Res* **2**: 595–610.

15) Hara K, Kobayasi M, Akiyama Y. 2002. Vitamin K_2 (menatetrenone) inhibits bone loss induced by prednisolone partly through enhancement of bone formation in rats. *Bone* **31**: 575–581.

16) Ortoft G, Oxlund H. 1996. Qualitative alterations of cortical bone in female rats after long-term administration of growth hormone and glucocorticoid. *Bone* **18**: 581–590.

17) Tanaka Y, Nakamura T, Nishida S, Suzuki K, Takeda S, Sato K, Nishii Y. 1996. Effects of a synthetic vitamin D analog, ED-71, on bone dynamics and strength in cancellous and cortical bone in prednisolone-treated rats. *J Bone Miner Res* **11**: 325–336.

18) Furuichi H, Fukuyama R, Izumo N, Fujita T, Kohno T, Nakamuta H, Koida M. 2000. Bone-anabolic effect of salmon calcitonin on glucocorticoid-induced osteopenia in rats. *Bio Pharm Bull* **23**: 946–951.

19) Nitta T, Fukushima T, Nakamuta H, Koida M. 1999. Glucocorticoid-induced secondary osteopenia in female rats: a time course study as compared with ovariectomy-induced osteopenia and response to salmon calcitonin. *Jpn J Pharmacol* **79**: 379–386.

20) Noa M, Mendoza S, Mas R, Mendoza N, Leon F. 2004. Effect of D-003, a mixture of very high molecular weight aliphatic acids, on prednisolone-induced osteoporosis in Sprague-Dawley rats. *Drugs R D* **5**: 281–290.

21) Ikeda S, Morishita Y, Tsutsumi H, Ito M, Shiraishi A, Arita S, Akahoshi S, Narusawa K, Nakamura T. 2003. Reductions in bone turnover, mineral, and structure associated with mechanical properties of lumbar vertebra and femur in glucocorticoid-treated growing minipigs. *Bone* **33**: 779–787.

22) Manolagas SC, Weinstein RS. 1999. New developments in the pathogenesis and treatment of steroid-induced osteoporosis. *J Bone Miner Res* **14**: 1061–1066.

23) Shiraishi A, Higashi S, Masaki T, Saito M, Ito M, Ikeda S, Nakamura T. 2002. A comparison of alfacalcidol and menatetrenone for the treatment of bone loss in an ovariectomized rat model of osteoporosis. *Calcif Tissue Int* **71**: 69–79.